

Fast, accurate, and precise detector simulation with vision transformers

Luigi Favaro ^{1*}, Andrea Giammanco ¹, Claudius Krause ²

¹ Centre for Cosmology, Particle Physics and Phenomenology (CP3), Université catholique de Louvain, Louvain-la-Neuve, Belgium

² Marietta Blau Institute for Particle Physics (MBI Vienna), Austrian Academy of Sciences (ÖAW), Vienna, Austria

* luigi.favaro@uclouvain.be



EuCAIF

*The 2nd European AI for Fundamental Physics Conference (EuCAIFCon2025)
Cagliari, Sardinia, 16-20 June 2025*

Abstract

The speed and fidelity of detector simulations in particle physics pose compelling questions about LHC analysis and future colliders. The sparse high-dimensional data, combined with the required precision, provide a challenging task for modern generative networks. We present a comparison between solutions with different trade-offs, including accurate Conditional Flow Matching and faster coupling-based Normalising Flows. Vision Transformers allows us to emulate the energy deposition from detailed GEANT4 simulations. We evaluate the networks using high-level observables, neural network classifiers, and sampling timings, showing minimum deviations from GEANT4 while achieving faster generation. We use the CaloChallenge benchmark datasets for reproducibility and further development.

Copyright attribution to authors.

This work is a submission to SciPost Phys. Proc.

License information to appear upon publication.

Publication information to appear upon publication.

Received Date

Accepted Date

Published Date

1 Introduction

Precision measurements and new physics discoveries at colliders rely on a controlled and accurate simulation chain from first principles to the detector-level observables. However, to match the size of experimental data collected in the future years, the amount of computing dedicated to simulations will exceed the available budget. Matching these requirements calls for novel, fast, and accurate simulation techniques. Modern machine learning emulators provide fast, yet precise, alternatives capable of modeling high-dimensional spaces.

In particular, generative networks are used to emulate and accelerate the calorimetric response in detectors, which often corresponds to the slowest component of the simulation

chain [1]. A neural network uses training data generated with detailed simulations such as GEANT4 [2] to approximately learn the distribution of calorimeter showers and provide an accessible way to sample from this space. In a large community effort, known as the CaloChallenge [3], many generative networks have been compared on a set of benchmark datasets. From such a study, 3D Vision Transformers emerged as a powerful network architecture to model calorimeter showers in a voxelised space. We focus on normalising flows, which provide faster sampling but with restrictions on the modelling of the data density, and continuous normalising flows trained with conditional flow matching, which provide more flexible transformation at the cost of slower sampling times. Our discussion on the CFM network is partially taken from CaloDREAM [4], a submission to the CaloChallenge that showed top-performing results in several metrics.

We perform a thorough evaluation of the generative networks in terms of the sampling time for a calorimeter shower on GPUs, and the fidelity of the generated showers. Our metrics include layer-wise high-level features and binary neural network classifiers for a holistic comparison against GEANT4 on high-level features and voxel-level energy depositions.

2 CaloChallenge datasets

For our studies, we use four public [5–7] datasets that have been used for the Fast Calorimeter Simulation Challenge [3]. They are GEANT4 simulations of a single particle showering in different calorimeters. The detector has a cylindrical shape with segmentation along the radial and angular directions. Each shower provides the incident energy of the incoming particle and the energy deposition in each voxel of the detector geometry.

The two samples contained in Dataset 1 (DS1) simulate central photons and pions. These simulations were already used for the training of ATLFAST3 [8]. These two datasets have irregular geometries with layer-wise segmentation in $r \times \alpha$:

$$\begin{aligned} \text{photons} & \quad 8 \times 1, 16 \times 10, 19 \times 10, 5 \times 1, 5 \times 1, \\ \text{pions} & \quad 8 \times 1, 10 \times 10, 10 \times 10, 5 \times 1, 15 \times 10, 16 \times 10, 10 \times 1, \end{aligned} \quad (1)$$

for a total of 368 and 533 voxels for photons and pions, respectively. The incident energies are a discrete set of values in $E_{\text{inc}} = 256 \text{ MeV} \dots 4.2 \text{ TeV}$, in powers of two.

Datasets 2 and 3 (DS2/3) instead assume a regular geometry with custom implementation in GEANT4. The detector has 90 layers of interleaved absorber and active material. Each pair is grouped into a single layer, totaling 45 voxel-level detector layers. The number of simulated electron showers is 100,000, produced at $\eta = 0$. The incident energy is log-uniformly sampled in $E_{\text{inc}} = 1 \dots 1000 \text{ GeV}$. The two datasets contain the same physics; they only differ in the voxelisation: in DS2 each layer is segmented into 16×9 angular and radial voxels, while a DS3 layer contains 50×18 voxels. More details on the GEANT4 simulations are available in [3].

3 Generative Vision Transformers

The generation process of a single shower is factorised into two parts, each modelled with a dedicated generative network. One “energy” network generates the total energy deposition in each layer, while a “shape” network generates the normalised voxel energy [9]. Expressed

in terms of energy-ratio features u_i , the energy network generates $p(u_i|E_{\text{inc}})$. The shape network is additionally conditioned on the truth energy ratios and learns $p(x|E_{\text{inc}}, u)$. The final sampling procedure follows

$$\begin{aligned} u_i &\sim p_\phi(u_i|E_{\text{inc}}) \\ x &\sim p_\theta(x|E_{\text{inc}}, u), \end{aligned} \quad (2)$$

where ϕ and θ are the learnable weights of the energy network and shape network, respectively. We study the trade-offs of two modern generative architectures: discrete Normalising Flows (NFs) [10] and Conditional Flow Matching networks (CFMs) [11]. Then, we describe the transformer-based architecture used for the shape network: a 3D Vision Transformer (ViT) [12, 13].

Generative networks

A normalising flow builds a map from the data space p_{data} to a simple latent space p_{latent} , typically Gaussian. We define the forward map, represented by a neural network, as $f_\theta(x)$. The loss function minimised in a normalising flow is then the negative log-likelihood defined as

$$\mathcal{L}_{\text{INN}} = -\left\langle \log p_{\text{latent}}(f_\theta(x)) + \log \left| \frac{\partial f_\theta(x)}{\partial x} \right| \right\rangle_{x \sim p_{\text{data}}}. \quad (3)$$

To directly minimise the logarithm of Eq. (3), normalising flows limit the family of possible transformations to invertible f_θ with a tractable Jacobian.

Given an N -dimensional input vector, coupling blocks reduce the computational cost of calculating the Jacobian to $\mathcal{O}(N)$ operations by constructing an upper-triangular matrix. In practice, this is achieved by transforming half of the input features in each block, followed by a random permutation of the inputs. High-expressivity of the neural network is ensured by defining f_θ as a binned rational quadratic spline (RQS) [10]. An RQS predicts the heights, widths, and derivatives of m bins. Hence, a neural network predicts a vector $f_\theta(x) \in \mathbb{R}^{(3m-1)\frac{N}{2}}$. These are processed with a Softmax function to ensure the correct normalisation. The rational quadratic spline, in each bin k , is a function of the input ξ of the form

$$f_k(\xi) = \beta_{0k} + \frac{\beta_{1k}\xi(1-\xi) + \beta_{2k}\xi^2}{\beta_{3k} + \beta_{4k}\xi(1-\xi)}. \quad (4)$$

The details of the parameterisations, including the calculation of the inverse and the Jacobians can be found in [10]. Such normalising flows, or invertible neural networks, allow for the sampling of a calorimeter shower in a single inverse pass and, therefore, they are noticeably fast generators.

A more expressive alternative is a CFM generative network. We limit the discussion of CFM networks to the essentials and refer to the original paper [11] and CaloDREAM [4] for the details. A CFM generative network is an example of a continuous normalising flow, which introduces a velocity field $v(x, t)$ to map between representation spaces. A neural network trains such that $v_\theta(x, t) \approx v(x, t)$, typically by minimising a simple mean squared error loss. However, as $v(x, t)$ is intractable, the minimisation is recast in terms of the conditional velocity field $v(x, t|x_0)$, with, for instance, a linear trajectory between the two spaces. While CFM networks are strictly more expressive than discrete normalising flows, sampling from a trained network requires solving the equation

$$x(t=1) = x(t=0) + \int_0^1 v_\theta(x, t) dt. \quad (5)$$

We use standard numerical solvers, such as the Runge-Kutta method, which evaluate the network several times, therefore slowing the sampling process.

Vision Transformers

The high dimensionality of voxelised calorimeter data makes it unfeasible to use a transformer architecture directly. To avoid building an attention matrix with N^2 scaling, we devise a patching scheme that collects predefined neighbouring voxels in a single patch. Embedded patches are then passed to several transformer blocks, which build attention matrices of size equal to the number of patches. The transformation inside a transformer block can be summarised as

$$\begin{aligned} x_h &= x + \gamma_h g_h(a_h x + b_h), \\ x_l &= x_h + \gamma_l g_l(a_l x_h + b_l), \end{aligned} \quad (6)$$

where g_h and g_l represent the multi-head self-attention and the feed-forward transformation, respectively [4]. The scaling parameters a , b , and γ are predicted during training and depend on t , E_{inc} , and the energy ratios u . A final layer projects back to the output of interest. In a NF, the output is a vector containing the parameters of an RQS for each transformed voxel, while in a CFM, we predict a velocity vector for each voxel of the detector geometry.

More details on the implementation of 3D vision transformers for the calorimeter data are available in CaloDREAM [4]. In the NF setting, half of the patches are used to predict the RQS parameters of the other half. In each coupling block, we transform both halves of the shower before randomly permuting the inputs. While multiple shuffling options are possible along the spatial dimension, we limit our study to permutations of entire patches, i.e. along the channel dimension. For DS1, we introduce additional voxels to match the binning of the segmented layers and allow for regular patching. While the numbers of additional bins can be reduced to the size of the single patch, we leave it to future work.

4 Results

Applications of generative networks for fast simulations rely on the trade-off between sampling speed and fidelity. Therefore, we evaluate the generative vision transformers in terms of generation time and accuracy compared to GEANT4. As the sampling time of the layer energies is a sub-leading term to the total generation time, we employ a more precise CFM generator for the u variables throughout the text.

Generation time

The evaluation of the sampling time can depend on several external factors such as hardware, code implementation, and throughput overheads. In this study, we report the timing for the forward pass of the neural network on a single A100 GPU with a batch size of 256. We also include the overhead of moving the data from the GPU to the CPU. Table 1 compares the sampling time of NF and CFM vision transformers. For NFs, we report the generation time for a single shower, while for CFMs, we provide timings for a single step of the RK4 solver. We observe that the quality of generated showers reaches a plateau after 20 RK4 steps, which corresponds to 80 function evaluations.

The number of steps needed for CFM networks can be further reduced by using Bespoke samplers [4, 14, 15], a method which preserves the optimality of initial training of the generative network.

	NFs		CFMs	
	[ms per shower]		[ms per shower]	
	full gen.	1 step RK4	full. gen	
DS1- γ	1.93(3)	2.32(3)	22.7(3)	
DS1- π^+	2.12(5)	2.76(3)	28.7(5)	
DS2	6.9(5)	2.8(1)	27.5(5)	
DS3	12.3(5)	7.7(5)	125(1)	

Table 1: Generation time for a single calorimeter shower evaluated on a single A100 GPU with batch size 256. For the NFs, we report the time needed to generate a full shower, while for the CFMs, we indicate timings for both the full generation and a single RK4 step. Using RK4, the generation accuracy converges after 20 steps.

Fidelity

A first assessment of the generation quality of the calorimeter shower looks at high-level features. In Fig. 1 we show the number of inactive voxels, defined as λ , and two shower shape observables. We selected the centre of energy and its width, defined as

$$\langle \eta \rangle = \frac{\eta \cdot x}{\sum_i x_i}, \quad \sigma_{\langle \eta \rangle} = \sqrt{\frac{\eta^2 \cdot x}{\sum_i x_i} - \langle \eta \rangle^2}, \quad (7)$$

at the layer with the largest average energy deposition as a representative set of all the high-level features.

A comprehensive evaluation of the generative network should take into account the high-dimensional correlations of a calorimeter shower. A neural network classifier trained to distinguish a GEANT4 sample from a generated one approximates the likelihood ratio of the two distributions, the optimal test statistic for a simple two-hypothesis test [9, 16]. Table 2 shows the area under the ROC curve (AUC) score for the networks trained on the CaloChallenge datasets. An AUC= 0.5 implies that the generated samples are indistinguishable from GEANT4. We report the results of a classifier trained on the full set of high-level features (HL) and on low-level (LL) calorimeter data. The classifier architecture and the training hyperparameters closely follow those used in [3]. We observe that the CFM network has lower AUC scores across the board, while the NF shows a deteriorating performance as the detector granularity increases.

Additional computer science-inspired metrics that measure the precision and coverage of the generative networks are explored in [3].

5 Conclusion

We demonstrated that Vision Transformers are powerful architectures for fast calorimeter shower generation. For fast simulation applications, there is a trade-off between sampling speed and accuracy, and the optimal solution likely depends on the problem at hand. We presented a fast sampling solution based on RQS normalising flows, which provides generated calorimeter showers in a single forward pass, and the more accurate continuous normalising flows trained with CFM, which can produce samples almost indistinguishable from GEANT4 at the cost of multiple forward passes needed for a single sample.

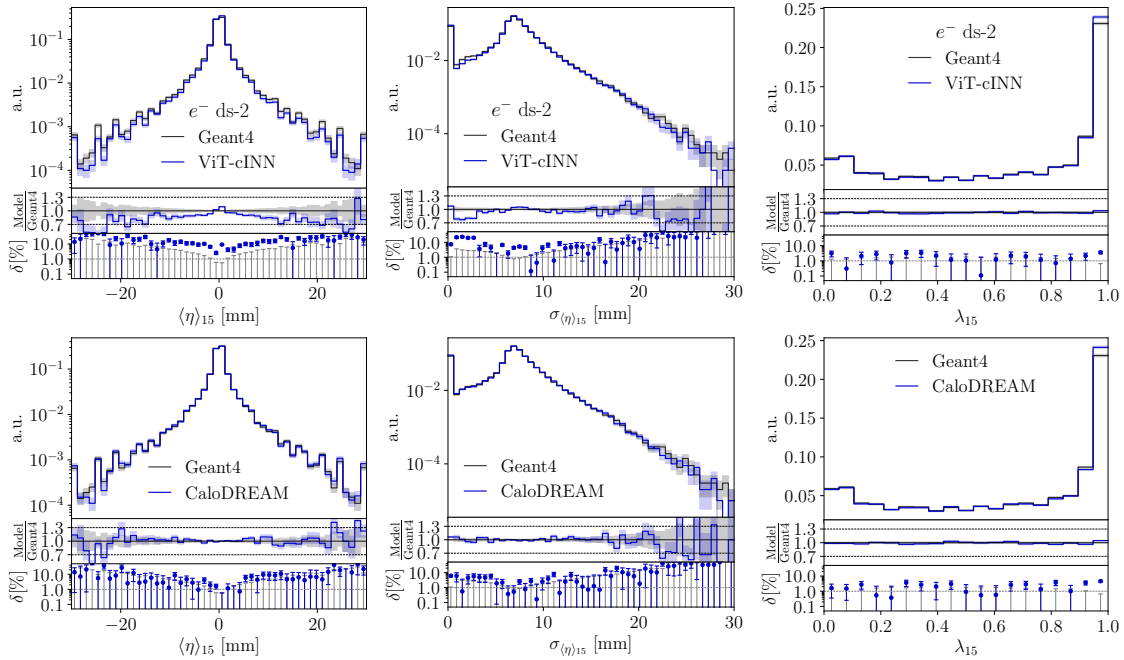


Figure 1: Set of high-level features for the NF (top) and the CFM (bottom) for DS2. From left to right, we show the center of energy, the width of the center of energy, and the sparsity of calorimeter shower in a single detector layer. CFM plots are reproduced from [4].

Our benchmarks, the CaloChallenge datasets, are public and available to the community for the future development of cutting-edge generative networks. The code is publicly available at the GitHub repository <https://github.com/luigifvr/vit4hep>. The same repository contains the configurations used to produce these results.

Acknowledgements

L.F. is supported by the Fonds de la Recherche Scientifique - FNRS under Grant No. 4.4503.16. The present research benefited from computational resources made available on Lucia, the Tier-1 supercomputer of the Walloon Region, infrastructure funded by the Walloon Region under the grant agreement n°1910247.

NFs	AUC		CFMs	AUC	
	LL	HL		LL	HL
DS1- γ	0.61	0.53	DS1- γ	0.51	0.51
DS1- π^+	0.74	0.60	DS1- π^+	0.63	0.52
DS2	0.68	0.78	DS2 [4]	0.53	0.52
DS3	0.64	0.84	DS3 [4]	0.63	0.52

Table 2: AUC scores from a classifier trained to distinguish GEANT4 from generated calorimeter showers. We train a classifier on high-level features (HL) and low-level energy depositions (LL) for NFs (left) and CFMs (right). The CFM results for DS2/3 are taken from [4].

References

- [1] S. Badger *et al.*, *Machine learning and LHC event generation*, SciPost Phys. **14**(4), 079 (2023), doi:[10.21468/SciPostPhys.14.4.079](https://doi.org/10.21468/SciPostPhys.14.4.079), [2203.07460](https://doi.org/10.21468/SciPostPhys.14.4.079).
- [2] S. Agostinelli *et al.*, *GEANT4 — a simulation toolkit*, Nucl. Inst. Meth. A **506**, 250 (2003), doi:[10.1016/S0168-9002\(03\)01368-8](https://doi.org/10.1016/S0168-9002(03)01368-8).
- [3] O. Amram *et al.*, *CaloChallenge 2022: A Community Challenge for Fast Calorimeter Simulation* (2024), [2410.21611](https://arxiv.org/abs/2410.21611).
- [4] L. Favaro, A. Ore, S. P. Schweitzer and T. Plehn, *CaloDREAM – Detector Response Emulation via Attentive flow Matching*, SciPost Phys. **18**, 088 (2025), doi:[10.21468/SciPostPhys.18.3.088](https://doi.org/10.21468/SciPostPhys.18.3.088), [2405.09629](https://doi.org/10.21468/SciPostPhys.18.3.088).
- [5] M. F. Giannelli, G. Kasieczka, C. Krause, B. Nachman, D. Salamani, D. Shih and A. Zaborowska, *Fast calorimeter simulation challenge 2022 - dataset 1 version 3*, <https://doi.org/10.5281/zenodo.8099322> (2023).
- [6] M. F. Giannelli, G. Kasieczka, C. Krause, B. Nachman, D. Salamani, D. Shih and A. Zaborowska, *Fast calorimeter simulation challenge 2022 - dataset 2*, <https://doi.org/10.5281/zenodo.6366271> (2022).
- [7] M. F. Giannelli, G. Kasieczka, C. Krause, B. Nachman, D. Salamani, D. Shih and A. Zaborowska, *Fast calorimeter simulation challenge 2022 - dataset 3*, <https://doi.org/10.5281/zenodo.6366324> (2022).
- [8] G. Aad *et al.*, *AtlFast3: The Next Generation of Fast Simulation in ATLAS*, Comput. Softw. Big Sci. **6**(1), 7 (2022), doi:[10.1007/s41781-021-00079-7](https://doi.org/10.1007/s41781-021-00079-7), [2109.02551](https://doi.org/10.1007/s41781-021-00079-7).
- [9] C. Krause and D. Shih, *Fast and accurate simulations of calorimeter showers with normalizing flows*, Phys. Rev. D **107**(11), 113003 (2023), doi:[10.1103/PhysRevD.107.113003](https://doi.org/10.1103/PhysRevD.107.113003), [2106.05285](https://arxiv.org/abs/2106.05285).
- [10] C. Durkan, A. Bekasov, I. Murray and G. Papamakarios, *Neural spline flows* (2019), [1906.04032](https://arxiv.org/abs/1906.04032).
- [11] Y. Lipman, R. T. Chen, H. Ben-Hamu, M. Nickel and M. Le, *Flow matching for generative modeling*, arXiv preprint arXiv:2210.02747 (2022).
- [12] A. Dosovitskiy, L. Beyer, A. Kolesnikov, D. Weissenborn, X. Zhai, T. Unterthiner, M. Dehghani, M. Minderer, G. Heigold, S. Gelly, J. Uszkoreit and N. Houlsby, *An image is worth 16x16 words: Transformers for image recognition at scale*, ArXiv [abs/2010.11929](https://arxiv.org/abs/2010.11929) (2020).
- [13] W. S. Peebles and S. Xie, *Scalable diffusion models with transformers*, 2023 IEEE/CVF International Conference on Computer Vision (ICCV) pp. 4172–4182 (2022).
- [14] N. Shaul, J. C. Pérez, R. T. Q. Chen, A. K. Thabet, A. Pumarola and Y. Lipman, *Bespoke solvers for generative flow models*, ArXiv [abs/2310.19075](https://arxiv.org/abs/2310.19075) (2023).
- [15] N. Shaul, U. Singer, R. T. Q. Chen, M. Le, A. K. Thabet, A. Pumarola and Y. Lipman, *Bespoke non-stationary solvers for fast sampling of diffusion and flow models*, ArXiv [abs/2403.01329](https://arxiv.org/abs/2403.01329) (2024).

[16] R. Das, L. Favaro, T. Heimel, C. Krause, T. Plehn and D. Shih, *How to understand limitations of generative networks*, SciPost Phys. **16**(1), 031 (2024), doi:[10.21468/SciPostPhys.16.1.031](https://doi.org/10.21468/SciPostPhys.16.1.031), 2305.16774.